

Heat Transport in Liquid Filled Tubes

R. Schmid,^A B. A. Pailthorpe^B and R. E. Collins^B

^A Department of Mechanical Engineering, University of Sydney,
Sydney, N.S.W. 2006.

^B School of Physics, University of Sydney,
Sydney, N.S.W. 2006.

Abstract

When heat is applied to a liquid filled tube, the liquid moves under buoyancy forces which arise from density variations. In long thin tubes, inclined at an angle to the horizontal, two counter-flowing streams of liquid are observed which extend over virtually the whole length. A simple one-dimensional model is developed in which an analysis of heat flows into and between the two streams is made. This is used to predict the temperature in the system and the average fluid velocities at any point in the tube. The results of the model are in good agreement with experimental measurements on these tubular systems, and on a planar convection cell. Systems such as this can exhibit very large effective thermal conductances, and may be useful as a heat extraction device in evacuated tubular solar collectors.

1. Introduction

Evacuated tubular solar collectors offer unique promise for the next generation of solar hot water systems. The Sydney University selective surface (Harding and Window 1979; Harding *et al.* 1982; Window and Harding 1984) has achieved a near optimum mix of high solar spectrum absorptance and low infrared emittance resulting in extremely low radiation losses. Heat losses by conduction and convection have been virtually eliminated by vacuum insulation. In order to utilise these devices in practical cost-effective systems it is necessary similarly to optimise the balance of system components. In particular, heat extraction from a single ended solar absorber (see Fig. 1) presents challenging problems. A variety of concepts have been canvassed in the literature already (Harding *et al.* 1985; Yin *et al.* 1985) and some are appearing in the market-place. Thermosiphoning tubes, in which hydraulic flows are driven by buoyancy forces alone, offer the prospect of efficient and cost-effective heat extraction. Until now, however, their operation has not been clearly understood. It turns out that the underlying hydrodynamics and heat transfer processes exhibit a surprising complexity and subtlety. Nevertheless, the practical performance characteristics of this heat extraction device can be described in simple terms.

In this paper we present a simple, essentially one-dimensional, theoretical model of heat extraction from solar collectors utilising liquid filled tubes. This model provides significant insight into the physics of the system and serves to correlate available data on thermosiphoning manifold temperature profiles in solar collectors. Two other experimental systems are also discussed, a cylindrical riser tube and a rectangular

convection cell, both of which are electrically heated. Study of thermosiphoning flows in these more controlled systems provides further insight into the mechanisms of operation. In particular, flow visualisation experiments are used to verify the basic assumptions of the simple model.

2. Convection—An Overview

The study of flows driven by buoyancy forces is a branch of hydrodynamics which offers scope for significant fundamental analysis, as well as wide application in modern technology and in the understanding of natural phenomena. Applications include heat exchanger design, fluid motions in the Earth's interior, the oceans and the atmosphere, and astrophysical phenomena. Turner's (1973) monograph gives a wide ranging coverage of the topic and its applications. Texts by Jaluria (1980), Holman (1981) and Gebhart (1971) provide illustrative and more specific studies of convection in technologically relevant systems.

Convection is known to have been studied in Antiquity, but the origins of the modern theory can be traced back just over one hundred years. For example, in 1881 Lorenz first calculated the heat transferred by convection from a hot vertical plate in still air, although Oberbeck had previously described the underlying physics (see Mihaljan 1962). Oberbeck also attempted one of the first meteorological studies. The physics of convection was again presented by Boussinesq (1903), whose name is now associated with the standard approximation in the study of convection. Flows are driven only by density differences, arising from existing temperature differences which do not otherwise enter the hydrodynamic equations of motion. Thus, fluid properties are assumed to be constant; in particular, the fluid is incompressible. This approximation, which significantly simplifies the analysis, is appropriate to most problems of practical interest. A possible exception occurs when very large temperature differences are present. For water, with a viscosity which varies by about a factor of 2 over a temperature range of 40°C, use of the Boussinesq approximation incurs an error of less than 15%. This is significantly reduced for smaller temperature differences. Perhaps the best known convective phenomena occurs in a fluid heated from below. Bénard (1901) and Rayleigh (1916) began the study of this system which can exhibit visually striking flow patterns, such as hexagonal convective cells. Subsequent studies of convection considered the flows near isolated hot surfaces and free plumes above hot spots. The application of natural convection principles to solar hot water systems is now well advanced.

Of more relevance to the present study, Batchelor (1954) considered the convective flow in a vertical cavity with isothermal walls, one side being hotter than the other. This work suggested the possibility of an isothermal core and identified the three dimensionless parameters characterising the flows. Lighthill (1953) presented a comprehensive analysis of the thermosiphoning tube (cylindrical cavity) placed vertically in strong gravitational fields. The analysis is relevant to the problem of turbine blade cooling which was also studied using the so-called 'open thermosiphon' concept during the 1950s. The open thermosiphon is conceptually very similar to a riser tube connected to a header of constant temperature (cf. Fig. 1*b*). In turbine blades, cylindrical fluid flow passages 'communicate' with a fluid reservoir of approximately constant temperature in the rotor drum. Experimental work on solar heating systems which include the study of the effect of inclination has been reported

by Martin and Cohen (1954), Martin (1955), Hartnett and Welsh (1957), Larsen and Hartnett (1961) and Hasegawa *et al.* (1963).

Significant experimental insight was provided by Elder's (1965a) study of the convection of silicone oil in a vertical rectangular cavity with isothermal walls. This work showed the existence of longitudinal temperature gradients in the fluid core and of boundary layer motions. Subsequently, Gill (1966) performed a boundary layer analysis on this system using the insights provided by Elder's experiments and successfully described the observed flows and temperature distributions. Convective flows in an inclined rectangular cavity, again with isothermal walls, were described by Hart (1971). Analogous flows in the horizontal cylinder with specified wall temperature profiles have also been extensively investigated (see Ostrach 1972). One of the few convection systems with constant heat flux boundary conditions, as in the present study, is the vertical box described by Kimura and Bejan (1984). In their system heat flows across the cell, as in previous studies involving isothermal boundaries.

An important development in the study of convection was the so-called thermosiphoning loop introduced by Keller (1966) and Welander (1967) and first comprehensively studied by Crevelling *et al.* (1975). In its simplest form the loop is a liquid filled toroidal cell (about the size of a bicycle inner tube) which is oriented vertically. The cell is uniformly heated over the lower half of the loop and cooled over the top half. The resulting convective flow can be steady, periodic, even multi-periodic, and ultimately chaotic, depending on the applied driving force. A single measurement of the temperature difference between opposite sides of the toroid (at 'three and nine o'clock') can be used to characterise the system.

Convective flows in the thermosiphoning loop may be analysed by a 'one-dimensional' set of Navier-Stokes equations (Crevelling *et al.* 1975). One attractive feature of this system is that the dynamics are relatively accessible to analysis (Grief *et al.* 1979). Two-dimensional studies (Mertol *et al.* 1982) have confirmed the essential features of the one-dimensional analysis—which nevertheless does not provide quantitative agreement with experiment. Similar ideas have been extended to study the performance of solar heating systems (Huang 1980; Mertol *et al.* 1981). Subsequently, Sen *et al.* (1985) showed that the Navier-Stokes equations for the thermosiphoning loop could be approximated by the three Lorenz (1963) equations derived from the study of instabilities in convective flow with confining walls, which in turn enabled numerical characterisation of the onset of chaotic flows. Gorman *et al.* (1984) have identified three chaotic flow regimes, highlighting the interesting dynamics exhibited by this simple system. Hart (1984) further described the dynamic transitions using a simple cubic equation and suggested that no stable oscillatory motions are allowed. The existence of such motions was attributed to the complex and sensitive frictional drag law observed in thermosiphoning loops (Crevelling *et al.* 1975). Gorman *et al.* (1986) have also examined the quantitative applicability of the Lorenz equations to this flow. The thermosiphoning loop offers, firstly, a simple model for the study of transient convective flows relevant to solar performance and, more fundamentally, it also offers a readily understandable system, with identifiable physical parameters, which exhibits chaotic dynamics.

The heat extraction from evacuated tubular collectors has been investigated in two systems. The simplest option is to fill the evacuated tube with water (Fig. 1a)

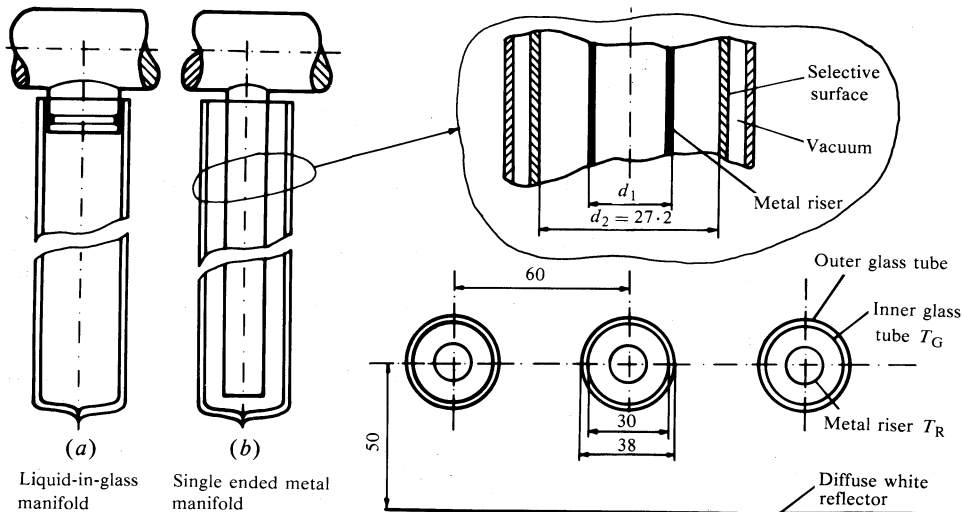


Fig. 1. Two heat extraction configurations used with evacuated tubular solar collectors: (a) thermosiphoning flow fills the evacuated tube and (b) thermosiphoning flow is confined to a concentrically mounted metal riser tube. In each case the flow 'communicates' via a header pipe or heat exchanger with a load or storage tank. The configuration of multiple evacuated tubes above a reflector is also illustrated. (All dimensions are in mm.)

which can thermosiphon via a header pipe to a storage tank. The performance of this 'fluid-in-glass' design has been characterised by Harding and co-workers (Window and Harding 1983; Window 1983; Yin *et al.* 1984; Harding and Yin 1985; Harding *et al.* 1985). A more robust design is to mount concentrically a liquid filled metal tube ('riser') inside an evacuated tubular collector (Fig. 1b), again with a common header pipe and possibly a heat exchanger. Performance data and temperature profiles have been obtained for this design (Yin *et al.* 1985; Schmid and Collins 1985). The primary aim of the present paper is to characterise the underlying convective flows in a thermosiphoning riser and to correlate these with observed temperature profiles. The influence of riser behaviour on system design and performance will be discussed elsewhere.

3. One-dimensional Model

To understand the experimental data and to delineate the parameters which control the thermal resistance of a thermosiphoning tube, we present a simple two-dimensional model. Consider a liquid filled tube (see Fig. 2) mounted at an angle ϕ to the horizontal and heated along its length. As a practical example, for an evacuated tubular collector mounted above a white diffuse reflector, the incident solar energy heats the tube uniformly along its length, but at different rates on the front and back surfaces. In this case, about two-thirds of the energy absorbed heats the upper side of the collector tube (\dot{Q}_2 in Fig. 2) and about one-third heats the lower side (\dot{Q}_1 in Fig. 2). More details of the geometry are shown in Fig. 1b.

As discussed in Section 2, several relevant systems have been extensively reviewed; in particular, convective flows in the vertical slot (Batchelor 1954; Elder 1965*a*;

Gill 1966) and in the inclined box (Hart 1971) with isothermal walls are fairly well understood. Primary circulation flows, secondary flow complexities and flow stability have been described experimentally and theoretically. In all cases heat flows across the cell from a hot to a cold wall and, consequently, the systems have a characteristic symmetry. Lighthill's (1953) work, however, did consider axial heat flow in a tube with isothermal walls. These studies provide significant insight into the present system with its constant heat flux boundary condition. An important difference in the present work is that heat is supplied to both sides of the cell and extracted at one end. The flows now exhibit a further symmetry which must be considered. Kimura and Bejan (1984) considered convection in a vertical box with constant heat flux boundary conditions, but again so that heat flows across the cell.

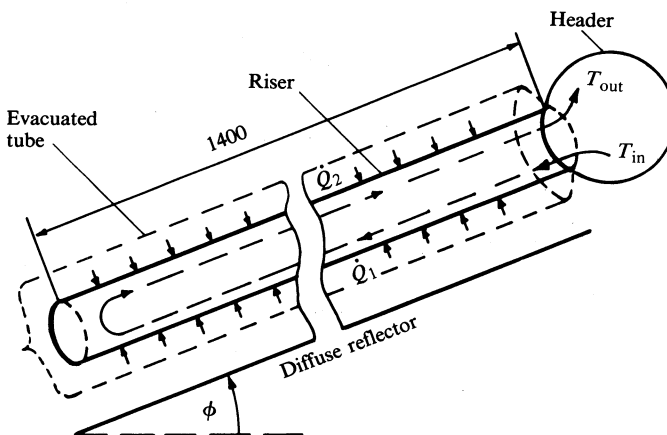


Fig. 2. Schematic diagram of a liquid filled thermosiphoning riser mounted inside an evacuated tube. Typical riser length is 1400 mm and internal diameter is 10 mm. Asymmetric heat fluxes \dot{Q}_1 and \dot{Q}_2 are applied to the bottom and top halves respectively of the riser. A stratified two-stream thermosiphoning flow, as shown, extracts heat from the riser to the header.

The flow pattern in a thermosiphoning tube has not yet been explicitly analysed, although some schematic representations have been presented (Window and Harding 1983). Flow visualisation experiments (see Section 5) indicate that at low heat fluxes the thermosiphoning flow in its simplest form is a single unicell; i.e. the flow proceeds as a single stream to the bottom of the tube and back in a single loop as shown in Fig. 2. There are no closed convection cells which might isolate parts of the absorber tube. The heat flux driving the flow is the controlling parameter. For larger heat fluxes (even within the 45 W power rating of evacuated tubular collectors) other flow patterns, and eventually turbulent flow, are observed; for example, closed convection loops appear and wave-like motions, as observed by Elder (1965b), may also be present. Temperatures measured on the metal tube walls are steady but, when measured in the flow, can exhibit oscillations and instabilities as in the thermosiphoning loop.

The simplest model of this flow is shown in Fig. 3. The downward flowing cold liquid stream and the upward flowing hot stream are, to a large extent, mechanically isolated from each other. There is of course a mutual viscous drag between the counter-flowing streams. In addition, there may be thermal conduction between the

two streams, either directly through the liquid or around the walls of the metal tube which contains the fluid. Mass exchange between the streams, with an associated heat transfer, is possible and may contribute at higher heat fluxes.

Inclination from the vertical of the thermosiphoning riser establishes the two stream flow since gravity acts to produce a stable stratification. For solar heating systems, an inclination ϕ equal to the latitude angle (34° for Sydney) provides the optimal average annual performance, although other inclinations such as the roof angle ($\approx 20^\circ$) are commonly adopted. A vertical riser ($\phi = 90^\circ$) exhibits a more complex flow with two coaxial streams or three planar streams being possible: hot liquid rises along the walls of the tube and cooler liquid descends in the core (see Lighthill 1953).

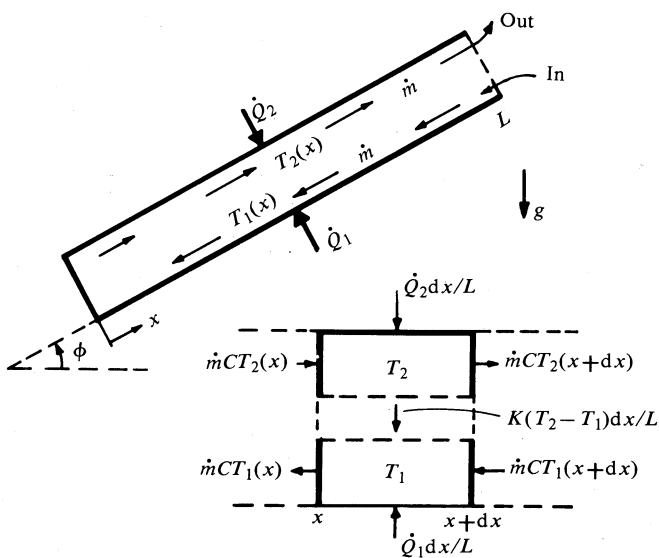


Fig. 3. Two-dimensional model of thermosiphoning flow in a riser showing counter-flowing streams characterised by average temperatures $T_1(x)$ and $T_2(x)$. The energy balance for a cross section of the tube, used to derive equations (1) and (2), is also shown.

As shown in Fig. 3, cool liquid enters the riser tube from a bath (the header) and is heated as it flows down and back up the riser to be ejected into the header. Heat extraction is almost exclusively by convection and longitudinal thermal conduction is negligible. In the steady state the in-out mass flux \dot{m} is constant. Mass conservation requires the up- and down-stream mass fluxes to be equal at each position x along the riser tube. Initially, leakage between the two streams is neglected so that \dot{m} is constant throughout the flow in the riser. The analysis is generalised below to include mass transfer between the streams.

The initial model developed is 'one-dimensional' in the sense that the fluid properties in each of the streams are considered to be a function only of the distance x from the lower end of the cell. The two axial counter-flowing streams are thus assumed to be characterised by average temperatures $T_1(x)$ and $T_2(x)$ for the lower (cooler) and upper (hotter) streams respectively. To relate the results of the model to the cylindrical tubes, the temperatures and flows can therefore be interpreted as (appropriately weighted) averages over half of the tube cross section.

Temperature Profiles

The temperature profiles can be characterised by a simple energy balance argument. Consider the volume elements in Fig. 3, taken as a cross-sectional slice from the riser. The energy flows in and out of each element, and conservation of energy yields two differential equations for the temperature profiles:

$$\frac{dT_1}{dx} + \frac{\dot{Q}_1}{\dot{m}CL} + \frac{K}{\dot{m}CL}(T_2 - T_1) = 0, \quad (1)$$

$$\frac{dT_2}{dx} - \frac{\dot{Q}_2}{\dot{m}CL} + \frac{K}{\dot{m}CL}(T_2 - T_1) = 0, \quad (2)$$

where C is the isobaric heat capacity of the liquid, K is an effective thermal conductance (in $\text{W}^\circ\text{C}^{-1}$) characterising heat exchange between the two elements, $d\dot{Q}_{12} = K(T_2 - T_1)dx/L$, and L is the length of the riser tube. The temperature difference between the two streams along the riser

$$\Delta T(x) = T_2(x) - T_1(x) \quad (3)$$

follows directly from (1) and (2):

$$\Delta T(x) = \frac{\dot{Q}_{\text{tot}}}{\dot{m}C} \frac{x}{L}, \quad (4)$$

where $\dot{Q}_{\text{tot}} = \dot{Q}_1 + \dot{Q}_2$ is the total heat supplied to the riser. Equation (4) can also be obtained directly by applying a calorimetric argument at any position along the riser.

Equation (4) enables direct integration of (1) and (2) and yields the temperature profiles

$$T_1(x) = T_1(0) - B_1 x - Ax^2 \quad (5)$$

$$= T_{\text{in}} + B_1(L-x) + A(L^2 - x^2), \quad (6)$$

$$T_2(x) = T_2(0) + B_2 x - Ax^2 \quad (7)$$

$$= T_{\text{out}} - B_2(L-x) + A(L^2 - x^2), \quad (8)$$

where

$$A = \frac{K\dot{Q}_{\text{tot}}}{2(\dot{m}CL)^2}, \quad B_1 = \frac{\dot{Q}_1}{\dot{m}CL}, \quad B_2 = \frac{\dot{Q}_2}{\dot{m}CL}, \quad (9, 10, 11)$$

$$T_{\text{in}} = T_1(L), \quad T_{\text{out}} = T_2(L). \quad (12)$$

Note that $T_1(0) = T_2(0)$ is required by energy conservation.

It is immediately apparent that heat transfer between the counter-flowing streams gives rise to temperature profiles which contain a quadratic, as well as a linear, component. The energy balance for the evacuated tube riser system follows from (6) and (9)–(12),

$$T_{\text{out}} - T_{\text{in}} = \dot{Q}_{\text{tot}}/\dot{m}C, \quad (13)$$

and can be used, for instance, to establish the mass flow rate \dot{m} .

The physical interpretation of these results is shown in Figs 4 and 5. Fig. 4 shows the effects of flux distribution on the two stream temperatures when there is no heat transfer between the two streams ($K = 0$). Two practical cases are shown, the first (Fig. 4a) illustrating flux conditions typically encountered in Sydney University evacuated tubular collectors incorporating a single-ended metal heat

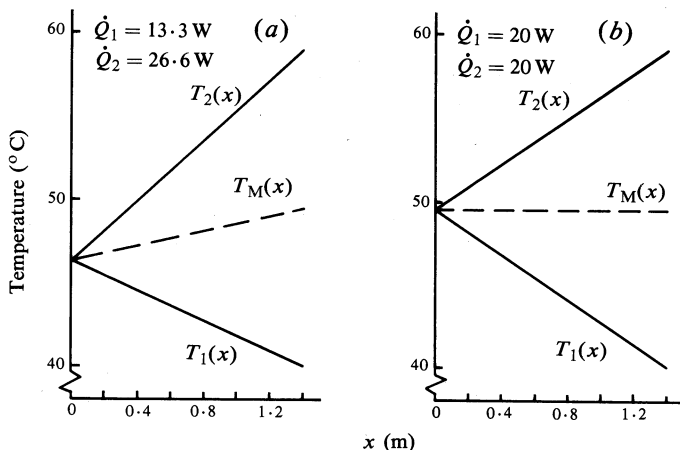


Fig. 4. Two stream temperature profiles for a riser tube calculated using equations (6)–(13) with no heat transfer between the two streams ($K = 0$). The effect of (a) asymmetric and (b) symmetric heating is shown. The average riser temperature T_M is also shown (dashed line).

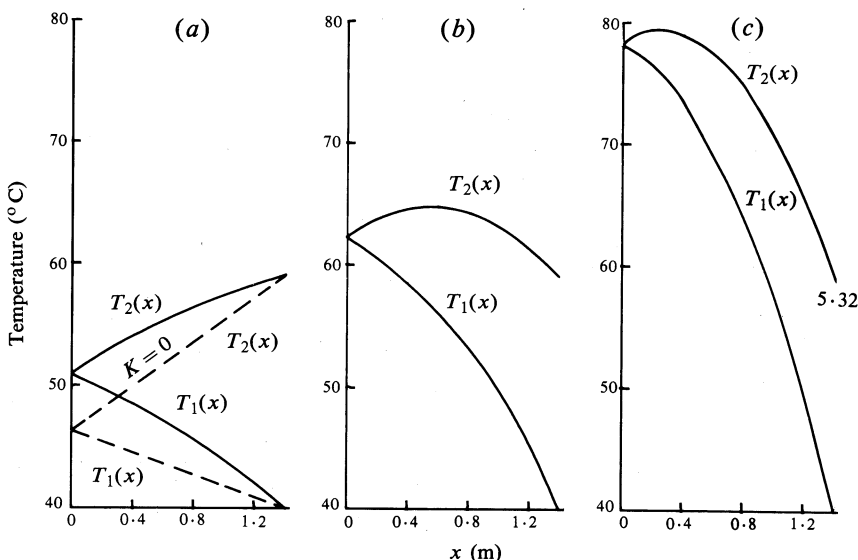


Fig. 5. Typical two stream temperature profiles predicted by equations (6)–(13) with heat transfer between the streams for the asymmetric heating case of Fig. 4b: (a) $K = 1$, (b) $K = 3.5$ and (c) $K = 7 \text{ W}^\circ\text{C}^{-1}$. The no heat transfer case ($K = 0$) is also shown (dashed line) for comparison.

extraction manifold and a white diffuse reflector. Approximately one-third of the total flux enters the riser through the bottom side and two-thirds through the top. Maximum thermal output of a single tube at a solar flux of 1000 W m^{-2} is typically 40 W per tube. It is worth noting that the slope of the mean fluid stream temperature is positive, in contrast to the measured temperature profiles (see Section 5), which suggests that there is conduction between the two counter-flowing streams.

Fig. 4b shows a case of equal fluxes into the top and bottom streams, as used in a number of indoor experiments. As the power to the top stream is increased, the mean stream temperature increases. In the absence of thermal conduction or mass exchange between the fluid streams, it appears that the lowest average riser temperature occurs where all power enters the riser from the top. This configuration would yield the highest average solar collector output. Note, however, that the case with no heat transfer between the top and the bottom stream ($K = 0$) is only relevant to other systems such as a U-tube manifold where the lower and the upper streams are physically separated.

The effect of stream conductance is shown in Fig. 5, where an asymmetric flux distribution similar to the case depicted in Fig. 4a is assumed. The first plot (Fig. 5a) shows a case of weak thermal coupling between the two streams. The shape of the temperature profiles $T_1(x)$ and $T_2(x)$ does not change significantly; however, the temperature at the closed end of the tube increases noticeably (by about 5°C) resulting in a change of the slope of the mean fluid stream temperature from positive to negative.

As the conductance K between the two streams is increased, the temperature at the closed end increases. In practice, this trend shows up clearly in measured temperature profiles in riser tubes of different materials. The low conductivity stainless-steel tube shows a moderate temperature gradient, whereas copper tubes exhibit larger temperature differences between the open and closed ends of the tube (Schmid and Collins 1985). Fig. 5b shows temperature profiles for a case with a conductance close to that for a water filled stainless-steel riser ($K \approx 4 \text{ W}^\circ\text{C}^{-1}$), while Fig. 5c illustrates the sensitivity of stream temperatures to changes in K .

In a typical riser tube configuration \dot{m} is determined by the hydrodynamics of the system and is therefore not a free variable. For Figs 4 and 5 we chose $\dot{m} = 0.5 \times 10^{-3} \text{ kg s}^{-1}$ which is typical for mass flow rates in inclined tubes with a diameter of order 10–15 mm.

Previous experiments often reported the average temperature profile along a thermosiphoning riser, which may be conveniently defined by

$$\bar{T}(x) = \frac{1}{2} \{ T_1(x) + T_2(x) \}, \quad (14)$$

and which, using (1), (2) and (4), can be derived from the differential equation

$$\frac{d\bar{T}}{dx} + \frac{K\dot{Q}_{\text{tot}}}{(\dot{m}CL)^2} x + \frac{\dot{Q}_1 - \dot{Q}_2}{2\dot{m}CL} = 0; \quad (15)$$

whence

$$\bar{T}(x) = \bar{T}(0) - \frac{\dot{Q}_1 - \dot{Q}_2}{2\dot{m}CL} x - \frac{K\dot{Q}_{\text{tot}}}{2(\dot{m}CL)^2} x^2. \quad (16)$$

It is apparent that the mean temperature gradient up the riser can be negative, consistent with heat flow to the top of the riser ($x = L$). The present system offers a practical realisation of a convection cell with an unstable axial temperature gradient, a situation previously unexpected (Gill 1966).

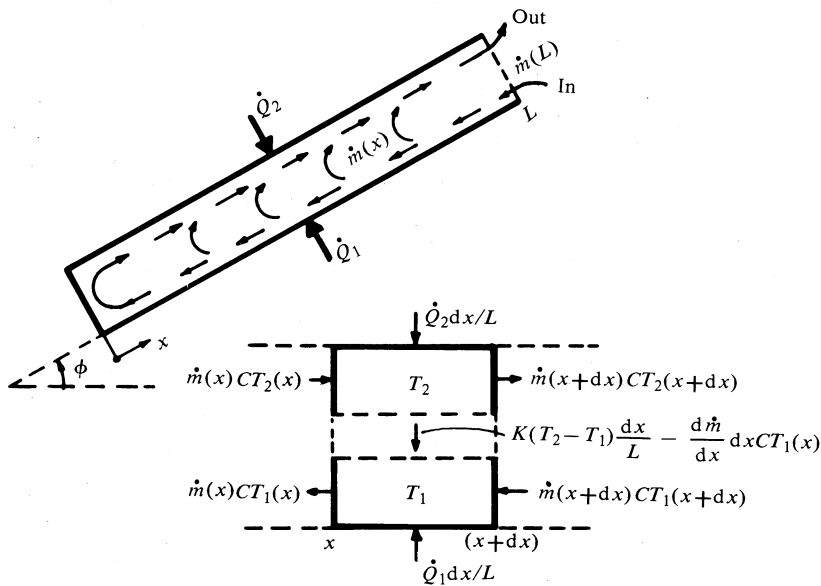


Fig. 6. Two-dimensional model of riser tube thermosiphoning flow with heat transfer and mass exchange between the two counter-flowing streams. The energy balance employed in deriving equations (17) and (18) is also illustrated. Note in particular that mass flow from the lower to the upper stream carries energy $(d\dot{m}/dx) CT_1(x) dx$.

The preceding analysis can be generalised to include mass exchange between the counter-flowing streams, as illustrated in Fig. 6. In this case exchange of fluid between the streams can occur and can be represented by writing the mass flow rate as an explicit function of x , i.e. $\dot{m}(x)$. Balancing energy flows through the volume elements shown in Fig. 6 yields, to first order,

$$\dot{m}(x) \frac{dT_1}{dx} + \frac{\dot{Q}_1}{CL} + \frac{K}{CL}(T_2 - T_1) = 0, \quad (17)$$

$$\dot{m}(x) \frac{dT_2}{dx} - \frac{\dot{Q}_2}{CL} + \left(\frac{K}{CL} + \frac{d\dot{m}}{dx} \right)(T_2 - T_1) = 0, \quad (18)$$

and these generalised differential equations reduce immediately to (1) and (2) when \dot{m} is independent of x . There are, however, only two equations in three unknowns. After straightforward algebra it is possible to derive a differential equation for the two stream temperature difference defined in (3):

$$\frac{d}{dx} \left(\dot{m}(x) \Delta T(x) \right) - \frac{\dot{Q}_{\text{tot}}}{CL} = 0. \quad (19)$$

Equation (19) can be immediately integrated to yield

$$\dot{m}(x) = \frac{\dot{Q}_{\text{tot}}}{CL} \frac{x}{\Delta T(x)}. \quad (20)$$

[This equation, similar to (4), can also be immediately derived from calorimetric arguments.]

Further progress is not possible without some knowledge of the mass flux profile $\dot{m}(x)$. This could be obtained experimentally from temperature profiles using (20) and will be discussed below. Alternatively we can seek an equation, in addition to (17) and (18), describing the mass exchange mechanism. In the absence of intuitive physical arguments, it is necessary to resort to a description involving a two-dimensional Navier-Stokes equation since the leakage flow $d\dot{m}/dx$ is, in fact, simply related to the cross tube liquid velocity. The full equations can be solved approximately using boundary layer analysis (Gill 1966) or numerical methods (Roache 1972).

Calculations

The choice of (6) and (8), for \dot{m} constant, or more generally (17) and (18) for fitting experimental temperature profiles can be decided by examination of the measured $\Delta T(x)$. A linear $\Delta T(x)$ plot intersecting the origin indicates \dot{m} is constant. This has been observed only for symmetric heating of the rectangular convection cell. Generally, we found that $\Delta T(x)$ is a concave function of x , although the data often appear linear away from the influence of end effects. Such linear fits do not intersect the origin, i.e. $\Delta T(x) \neq 0$ at $x = 0$. This is inconsistent with energy conservation and indicates that \dot{m} is a function of x .

When required, the functional form of $\dot{m}(x)$ can be extracted from the data by using (20). In all cases we found that the functional form of $\dot{m}(x)$ in (20), with

$$x/\Delta T(x) \approx px^s, \quad (21)$$

provides a good fit to the data. Some insight is provided by a simple calculation in which the hydrostatic driving force is equated to the (Poiseuille) viscous pressure drop for the flow in Fig. 6. Then we have $s = 0$. With (21), equations (17) and (18) may be integrated directly to yield

$$T_1(x) = T_1(0) - B_1 x^{1-s} - Ax^{2-2s}, \quad (22)$$

$$T_2(x) = T_2(0) - B_2 x^{1-s} - Ax^{2-2s}, \quad (23)$$

where

$$B_1 = \frac{\dot{Q}_1}{\dot{Q}_{\text{tot}}} \frac{1}{(1-s)p}, \quad B_2 = \frac{\dot{Q}_2}{\dot{Q}_{\text{tot}}} - s \frac{1}{(1-s)p}, \quad A = \frac{K}{\dot{Q}_{\text{tot}} p^2 (2-2s)}. \quad (24, 25, 26)$$

Flow Stability

We propose a simple criterion from which progress can be made in determining the conditions under which the fluid separates effectively into two counter-flowing streams. We consider the mechanical energy involved in this separation and flow over a short length, compared with the situation where there is no separation and flow but

where the fluid contains the same amount of thermal energy. The mechanical energy consists of two terms, the kinetic energy (positive) and the potential energy (negative, since the upper stream is of lower density). If this net energy difference is negative, it is energetically favourable for the separation and flow to be established. If positive, separation and flow will not occur since this would increase the total mechanical energy of the system. This analysis, therefore, can show the possibility of any isolated convection cells which might occur near the closed end of the riser.

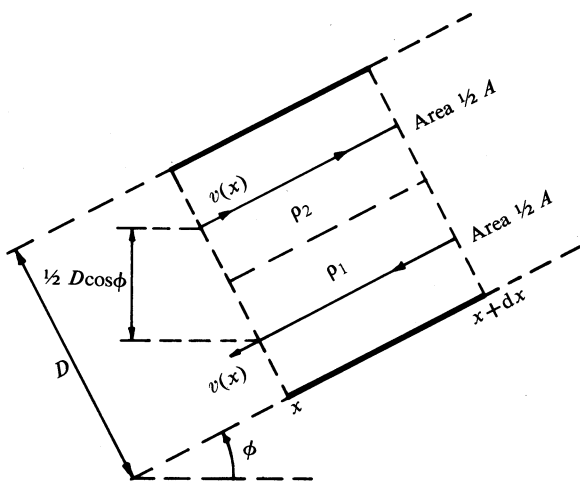


Fig. 7. Illustration of the energy based discussion, using equations (27) and (28), of two stream stability in thermosiphoning riser flow.

We consider the volume elements shown in Fig. 7 which represent a cross-section slice of area A and thickness dx taken at a distance x along the riser of Fig. 3. We calculate the difference in mechanical energy between the situation where the flow pattern is established, with an associated temperature difference between the streams, and that where the liquid is static and the temperature uniform. The kinetic energy of the two liquid streams between x and $x+dx$ is

$$KE = \frac{1}{2}\rho_1 \frac{1}{2}A dx \overline{v^2(x)} + \frac{1}{2}\rho_2 \frac{1}{2}A dx \overline{v^2(x)} \approx \frac{1}{2}\bar{\rho} A \overline{v^2(x)} dx, \quad (27)$$

where $\overline{v^2(x)}$ is the mean square fluid speed in each stream and $\bar{\rho} = \frac{1}{2}(\rho_1 + \rho_2)$ is the average liquid density. The extra gravitational potential energy associated with stratification of the two fluid elements is

$$PE = \{\rho_2(x) - \rho_1(x)\} \frac{1}{2}A dx g \frac{1}{2}D \cos \phi, \quad (28)$$

where g is the gravitational constant, D the diameter and ϕ the inclination of the riser. Stable stratification of the counter-flowing streams requires

$$PE + KE < 0 \quad (29)$$

since, under this condition, the stratified case with fluid flow is a state of lower mechanical energy. With (27) and (28), this condition may be written as

$$\rho \overline{v^2(x)} + \{\rho_2(x) - \rho_1(x)\} \frac{1}{2} D g \cos \phi < 0. \quad (30)$$

The Boussinesq approximation provides the density difference to first order:

$$\{\rho_2(x) - \rho_1(x)\}/\bar{\rho} = -\beta \Delta T(x), \quad (31)$$

where the isobaric thermal volumetric expansion coefficient is

$$\beta = -\frac{1}{\rho} \left(\frac{\partial \rho}{\partial T} \right)_P, \quad (32)$$

which for water is typically $5 \times 10^{-4} \text{ } ^\circ\text{C}^{-1}$. To first order v is independent of x and can be found from the mass flux

$$\dot{m} = \frac{1}{2} A \bar{\rho} v,$$

which in turn may be approximately calculated by using Poiseuille's law (Hansen 1967),

$$\dot{m} = \frac{\pi \rho a^4 \Delta P}{8 \mu (2L)}, \quad (33)$$

where a is the equivalent hydraulic radius for half the riser ($a = D/2\sqrt{2}$), P is the pressure head driving the flow, μ is the liquid viscosity and the effective pathlength is approximately twice the riser length. The pressure head is simply related to the density difference at the top of the riser:

$$\Delta P = \frac{1}{2} (\rho_{\text{in}} - \rho_{\text{out}}) g L \sin \phi = \frac{1}{2} \beta \rho_{\text{in}} g L \sin \phi (T_{\text{out}} - T_{\text{in}}). \quad (34)$$

Thus, the average fluid velocity is

$$v = \frac{a^2 \Delta P}{8 \mu L} = \frac{D^2 \Delta P}{64 \mu L}. \quad (35)$$

Equation (30) with (31) and (33) becomes

$$2D^3 \beta g \rho_{\text{in}}^2 \left(\frac{\sin \phi (T_{\text{out}} - T_{\text{in}})}{128 \mu L} \right)^2 - \cos \phi \Delta T(x) < 0.$$

In other words, the flow is stable at position x if the temperature profile satisfies

$$\Delta T(x) > 2D^3 \beta g \rho_{\text{in}}^2 \frac{\sin^2 \phi}{\cos \phi} \left(\frac{T_{\text{out}} - T_{\text{in}}}{128 \mu L} \right)^2. \quad (36)$$

Turning points in the flow, i.e. the boundaries of convection cells, can be located by imposing an equality on (36).

The applicability of Poiseuille's law (33) to the present system is not obvious since observations of the frictional drag law in the thermosiphoning loop (Crevelling *et al.* 1975) indicate a possibly more complex relationship. For laminar convective flow, the friction factor (Hansen 1967) is larger than usually observed in Poiseuille flow by a factor of about 3.6. In addition, the onset of turbulent flow is observed at a Reynolds number of 1500 (corresponding to heat fluxes of about 1 kW m^{-2}), rather than 2300 as is usual in Poiseuille flow. These complications will be explored in future work.

Nevertheless, application of (36) to a typical experiment (11 mm inside diameter stainless-steel riser—see Section 4) indicates that the flow is stably stratified when $\Delta T(x) > 1.3^\circ\text{C}$. Thus, if the observed ΔT is less than about 1.3°C at some distance along the riser, the above argument predicts that the flow will turn there rather than at the bottom end of the riser. A separate convection loop is then possible in the lower portion of the riser. Since this will affect the efficiency of heat extraction, equation (36) serves as a guide in the design of thermosiphoning risers for use with evacuated tubes.

Thermal Impedance

It is also possible to derive a simple relationship between \dot{Q}_{tot} and $\Delta T(L) = T_{\text{out}} - T_{\text{in}}$ by considering the hydraulic impedance of the thermosiphoning riser. We recall that the mass flow rate \dot{m} in each stream is related to $\Delta T(L)$ by the simple calorimetric relationship (13). Now Poiseuille's law (33) yields \dot{m} in terms of the hydrostatic pressure head which in turn arises from $\Delta T(L)$, as given by (34). Thus, we have

$$\dot{m} = \Delta T(L)/Z, \quad (37)$$

where the characteristic impedance of the riser tube is

$$Z^{-1} = \pi \rho^2 a^4 \beta g L \sin \phi / 32 \mu L. \quad (38)$$

Finally, using (13), we have the desired result

$$\dot{Q}_{\text{tot}} = C \{\Delta T(L)\}^2 / Z, \quad (39)$$

which provides one measure of the thermal impedance of the thermosiphoning riser. Alternatively, the mass flow rate may be calculated from

$$\dot{Q}_{\text{tot}} = CZ\dot{m}^2. \quad (40)$$

The thermosiphoning riser tube is amenable to study by a variety of approaches. The two-dimensional, or lumped parameter, analysis presented above offers direct physical insight without the difficulties and uncertainties associated with analytic or numerical approximation schemes. The simplified theory was suggested by the available experimental evidence; however, ultimately the theory must be assessed in terms of experiment (see Section 5). It is also possible to assess the simple model by considering the full hydrodynamic equations of motion for convection in a uniformly heated riser tube.

4. Experiment

The need for understanding the operation of liquid filled risers arose for a practical reason—the desire to develop an efficient, inexpensive heat transfer system for evacuated solar collector tubes. Early in this work, our understanding of this system was largely empirical and based on the operation of prototype solar collectors incorporating collector tubes and risers. It was therefore natural that experimental techniques using the Sun as an energy source were initially developed as the diagnostic tool to understand the basic principles of operation. Eventually, the limitations of outdoor testing led to the development of alternative laboratory testing techniques; however, much of our understanding of the basic heat transport processes in liquid filled risers had already come from outdoor testing.

The two basic experimental techniques used to evaluate the performance of liquid filled risers are shown in Figs 8 and 9. In the first method, three Dewar-type evacuated collector tubes were mounted above a diffuse white reflecting background in a manner identical with the arrangement of the tubes (20–30) in an actual solar collector. All measurements were made on the centre tube; the other two were present to provide standard optical conditions for the incident solar energy. The tubes and reflector were placed on a rotating table inclined at the desired angle to the horizontal (usually the solar declination angle) and mechanically tracked to follow the Sun. With this arrangement, approximately three to four hours of data could be obtained around solar noon on a completely clear day. The solar energy input to the system was constant over a period of any measurement to within a few per cent. Small fluctuations in solar input tended to be damped by the thermal mass of various system components. The incident energy flux could be reduced by the use of shade cloths mounted above the collector tubes.

The solar collector tubes contain a selective surface (with high absorptance and low emittance) on the outer surface of the inner tube. Combined with the vacuum insulation in the space between the tubes, this results in very low thermal losses from the tubes. Most of the energy absorbed from the Sun is therefore transferred from the selective surface through the inner glass tube to a liquid filled metal riser mounted within the collector tube. This heat transfer process is also of critical importance to the operation of solar collectors and is the subject of a separate study. A characterisation of the mechanisms of this heat transfer process (conduction and radiation) and of the thermal properties of the evacuated tube made it possible to determine accurately the total energy absorbed by the evacuated tube and the losses from the collector tube under any particular experimental conditions. Thus, the net energy transported by the liquid filled riser could be measured, although somewhat indirectly. The arguments leading to this determination will be presented elsewhere.

The outdoor experiment contained one further feature which complicates the analysis, but which is an intrinsic part of the system: the incident energy is non-uniformly distributed around the circumference of the evacuated tube. This feature has been the subject of considerable analysis. It has been shown (Yin *et al.* 1984) that under clear conditions at normal incidence, approximately two-thirds of the input energy is incident on the upper surface of the tube and one-third on the lower surface for this experimental configuration. The circumferential distribution of energy on the selective surface is probably similar to the distribution reaching the inner riser. With this experimental technique, however, there is always a fairly large uncertainty in the

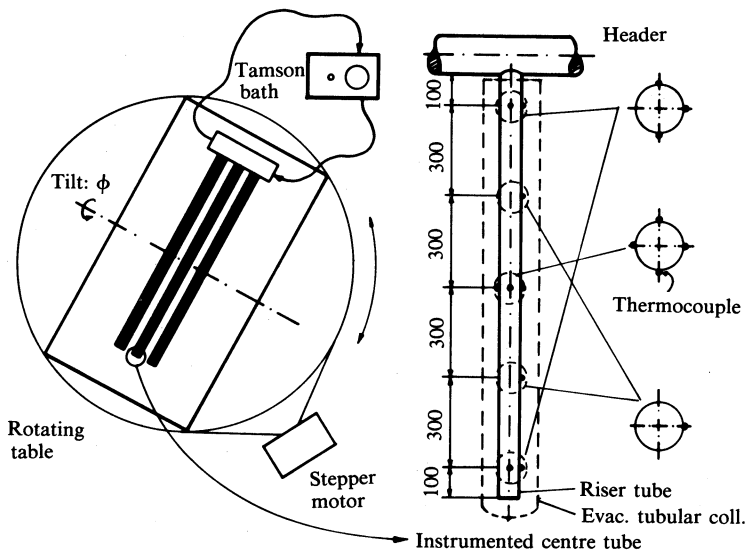


Fig. 8. Outdoor test rig comprising three evacuated tubes with a stainless-steel riser-header manifold mounted above a diffuse white reflector (as illustrated in Fig. 1). The collector is tilted at an angle ϕ to the horizontal (normally 34°) and tracks the Sun. The header pipe is maintained at constant temperature with a temperature controlled (Tamson) bath. The wall temperature of the centre tube is measured with thermocouples mounted as shown.

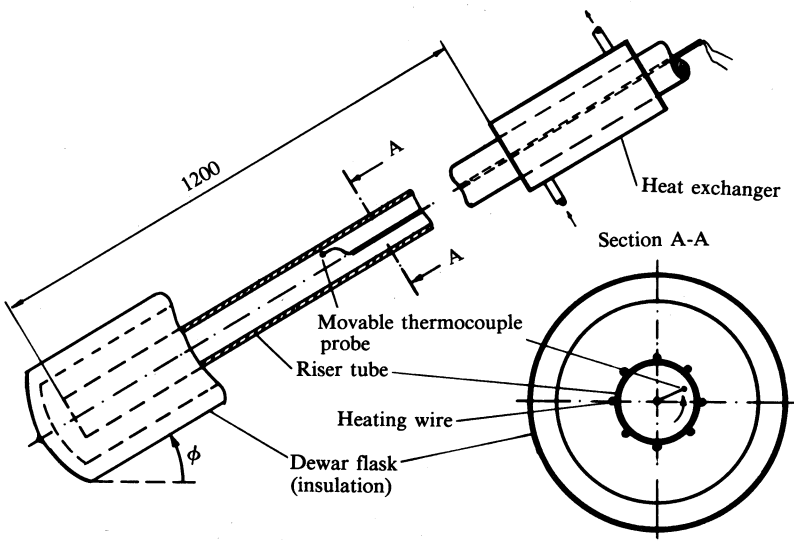


Fig. 9. Indoor test rig comprising an electrically heated riser tube (stainless steel or copper) which is vacuum insulated and cooled near its open end with a concentric heat exchanger. Cooling water is provided by a Tamson bath. A movable thermocouple probe was used to measure temperatures in the flow about 2 mm from the riser wall.

way this energy is distributed around the circumference of the riser and there is no straightforward method of measurement.

The difficulties in outdoor testing prompted the development of an alternative technique for injecting energy into a riser, as shown in Fig. 9. Heating wires, aligned along the riser and spaced uniformly around the circumference, were bonded to the riser surface with a thin layer of epoxy resin. Usually eight wires are attached to a tube of nominal diameter 13 mm (13.3 mm outside and 11.1 mm inside). Alternatively, the heating wires could be wound helically around the riser tube. The wires are electrically insulated from the tube by their thin polymer coating, but are in good thermal contact. Power is supplied to the system by passing electric current through the wires.

The advantages of this system are that the input energy can be defined precisely and held constant to high accuracy. The circumferential distribution of incident energy can be set as desired. The non-continuous spatial distribution of input energy is avoided as a result of the smoothing effect of the riser wall, particularly for high thermal conductivity metal risers. This system can be well insulated, resulting in most of the input energy entering the riser.

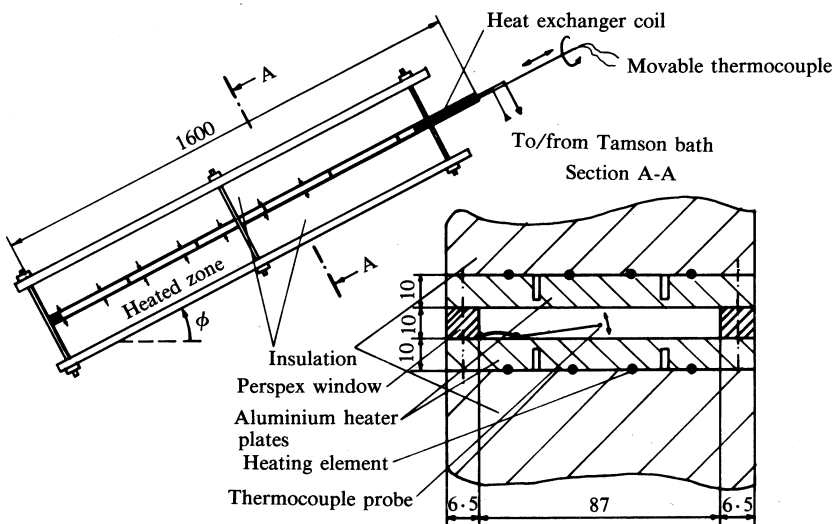


Fig. 10. Side view of a convection cell showing a $1600 \times 90 \times 10$ mm water filled cavity bounded above and below by precision machined aluminium heater plates with embedded heater elements and insulated with isocyanurate foam. The two outer 'guard' heaters on each plate are thermally isolated by slots from the central 'driver' heaters. Separate adjustment of power to the guards ensures constant heat flux across the cell. The fluid space is confined by perspex windows on the front and back sides. A movable thermocouple probe facilitates temperature measurements across and along the central region of the cell.

A third system investigated consists of an electrically heated rectangular convection cell of large aspect ratio (see Fig. 10). The flow is confined by narrow perspex spacers (10–17 mm) between two anodised aluminium plates ($1600 \times 110 \times 10$ mm) each of which is heated by four resistive strip heaters (1100 W, 1.1 m overall length, with 900 mm heated zone). The flow when laminar, i.e. for heat fluxes $< 500 \text{ W m}^{-2}$, appears

to be essentially two-dimensional with no significant three-dimensional features. Such a flow is amenable to a full theoretical treatment. Analogous flows have been observed in rectangular cavities with isothermal walls (Elder 1965*a*). Other flow modes are possible if the system is not carefully prepared; these modes will not be discussed here. The rectangular convection cell provides a well defined test for the theory of Section 3 without any complications associated with cylindrical geometry. This experimental system will be described more fully elsewhere.

The electrical heating method possesses another advantage in that a riser can be built from a clear material and standard techniques used to examine directly the flow behaviour within the riser. Polystyrene beads (<0.1 mm diam.) suspended in the flow, dye injection and a pH indicator technique (Baker 1966) have each been used to observe flow patterns and to estimate velocities, in a glass riser tube and in the rectangular cell. Distilled water was used as the heat transfer fluid in all indoor experiments and tap water for the outdoor experiments.

The above discussion deals with the two experimental methods used to supply energy to the riser. The rest of the apparatus is for extraction of energy from the riser. As a generalisation, in the present study we are more interested in the behaviour of heat flow along the riser, and less concerned with the complex effects associated with injection and extraction of fluid at the top end. It should be noted, however, that injection and extraction of fluid into and out of the top of the riser, and the temperature differences associated with this process, are quite important for the operation of solar collectors using liquid filled risers. It was found that stable operation of risers could be obtained by utilising many different methods to inject and extract fluids.

Two different methods have been used to inject and extract fluid. In one case, shown in Figs 1 and 8, the riser is connected directly into a horizontal header pipe through which fluid flows at constant temperature. In the other method, fluid is pumped down the riser through a small tube and drains at an outlet placed above the point of injection. In both cases, only a very small proportion of the fluid supplied to the riser participates in the heat transfer process over the whole length of the riser. The end effects involved in fluid injection and extraction into and out of the thermosiphoning loop are complex and have not been studied in any detail.

In the laboratory systems, heat exchangers (as in Fig. 9) were found to yield more stable conditions than those with fluid injection configurations. With fluid injection it was found that the system often reached a steady state only after many hours. In addition, at higher heat fluxes, and particularly as the system approaches the laminar-turbulent transition, oscillatory flows may be evident. The use of heat exchangers significantly reduced such problems and eliminated them completely well within the laminar flow regime. The time constant of the convection cell was then about one hour, consistent with the thermal conduction time constant for a quiescent body of water of equivalent scale. All data reported were recorded with stable steady state conditions ($\pm 0.1^\circ\text{C}$) evident over many hours for each experimental configuration.

Temperatures in these systems were measured by thermocouples (Chromel-Alumel) attached to the inner surface of the inner glass tubes of the evacuated tubular collector (for the outdoor test), and to the outer riser surface. In addition, movable thermocouples (tip diameter ≈ 0.05 mm) were utilised to probe the temperatures at various points within the fluid stream. These thermocouples were fed into the system

through a port at the top of the riser and manipulated from outside. Temperatures were recorded by hand with a Keithley (model 871) digital thermometer or by data loggers [Kaye Instruments Digistrip II for outdoors tests and a Data Electronics (Aust.) DT100 Datataker for indoors] with appropriate temperature reference points. The readings were averaged over periods of 15–60 min for outdoor and 5 s to 5 min for indoor.

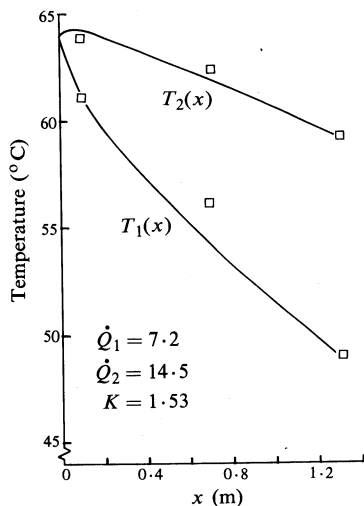


Fig. 11. Measured top and bottom wall temperatures (squares) for stainless-steel riser tubes heated by solar radiation on the outdoor test rig. The collector was tilted at 34° to the horizontal; the total input power was 21.7 W with $\dot{Q}_2 \approx 2\dot{Q}_1$. The curves represent the temperature profile predicted by equations (22) and (23).

5. Results

Experimentally determined temperature profiles for each of the three systems described in Section 4 are presented here and compared with the model and theory discussed in Section 3.

Evacuated Tube-Riser System (Outdoors)

Longitudinal temperature profiles were recorded for numerous riser tube configurations, tilt angles and solar fluxes (Schmid and Collins 1985). Note that with solar heating we have $\dot{Q}_2 \approx 2\dot{Q}_1$. In these experiments wall temperatures only were recorded at different locations on the circumference of the tube (top-sides-bottom cf. Fig. 8). The use of wall rather than fluid temperatures in determining model parameters such as the average mass flow rate is justified as follows. Measurements of temperature profiles across the inclined rectangular convection cell (cf. Figs 10 and 14*b*) indicate that $\Delta T(x)$ is well approximated by the difference in wall temperatures. Furthermore, with constant heat flux boundary conditions and laminar flow, the average stream temperature and $T_{\text{wall}}(x)$ have an approximately constant difference. We thus expect the wall temperatures to approximate the average fluid stream temperatures to within a constant offset. For asymmetric heating, however, this argument loses validity.

Typical measured wall temperatures for a stainless-steel riser mounted on the outdoor test rig (Fig. 8) are presented in Fig. 11. Theoretical fluid temperatures, calculated using (22) and (23), are shown for comparison. The mass flow rate $\dot{m}(x)$ is calculated from the experimental $\Delta T(x)$ using (21) and the parameters listed in Table 1. The remaining variable of the theory is K , the thermal conductance between

Table 1. Values of parameters in equations (21)–(23) used to fit the experimental temperatures in Figs 11–15

Fig.	System ^A	\dot{Q}_1 (W)	\dot{Q}_2 (W)	p	s	K ($\text{W}^\circ\text{C}^{-1}$)
11	SS	7.2	14.5	0.111	0.53	1.53
12a	SS	6.9	6.9	0.117	0.37	1.6
12b	SS	10.2	10.2	0.103	0.38	1.4
12c	SS	17.4	17.4	0.081	0.42	1.27
13a	Cu	7.3	7.3	0.084	0.33	3.8
13b	Cu	10.5	10.5	0.100	0.32	3.9
13c	Cu	14.8	14.8	0.082	0.33	3.9
14a	Cell	13.0	13.0	\dot{m} constant		35
15a	Cell	4.8	17.5	0.79	0.35	5.2
15b	Cell	0	20.2	1.03	0.27	15.6

^A SS, stainless-steel riser; Cu, copper riser; Cell, rectangular convection cell.

the two streams. The fitted K value of $1.5 \text{ W}^\circ\text{C}^{-1}$ compares with an estimate of $4 \text{ W}^\circ\text{C}^{-1}$ for the composite thermal conductance of a representative layer of water and riser tube wall.

Electrically Heated Glass Riser

The assumption of a two stream thermosiphoning flow pattern underlies the model discussed in Section 3. A glass riser tube, heated identically to the metal risers in Fig. 9, facilitated direct observation of the flow patterns. At low heat fluxes (of order 10^2 W m^{-2}) stable, stratified, approximately double Poiseuille profile flows were observed. Typical maximum velocities of order 1 cm s^{-1} were observed visually. At higher heat fluxes ($>500 \text{ W m}^{-2}$) turbulent convection became apparent, but the flow still retained the characteristic counter-flowing stream configuration.

Electrically Heated Metal Riser

Figs 12 and 13 show typical upper and lower stream temperatures measured in the electrically heated stainless-steel and copper risers using the apparatus in Fig. 9. Note that these risers are symmetrically heated ($\dot{Q}_1 = \dot{Q}_2$). The temperatures were measured in the flow about 2 mm from the top and bottom of the riser wall. Plots of $\Delta T(x)$ versus x were approximately linear only for $x > 0.2 \text{ m}$ and did not intersect the origin, so that \dot{m} will not be constant. Theoretical temperature profiles, calculated using (22) and (23), were fitted to the data using the K values shown in Figs 12 and 13 and the parameters listed in Table 1. There is some variation in K with changing heat flux. Nevertheless, the simple model described in Section 3 is able to predict temperature profiles in thermosiphoning risers given $\dot{m}(x)$ and some adjustment of a single parameter.

Electrically Heated Rectangular Cavity

Temperature profiles measured in the rectangular convection cell (Fig. 10) are shown in Figs 14 and 15. The first set of data (Fig. 14) is for symmetric heating ($\dot{Q}_1 = \dot{Q}_2 = 13 \text{ W}$) at a relatively low power level corresponding to a heat flux of about 150 W m^{-2} . This ensures that the flow is laminar and well removed from any transitions to turbulent flows. Visually observed fluid velocity exhibited characteristic double Poiseuille flow profiles with zero velocity at approximately the mid-plane of

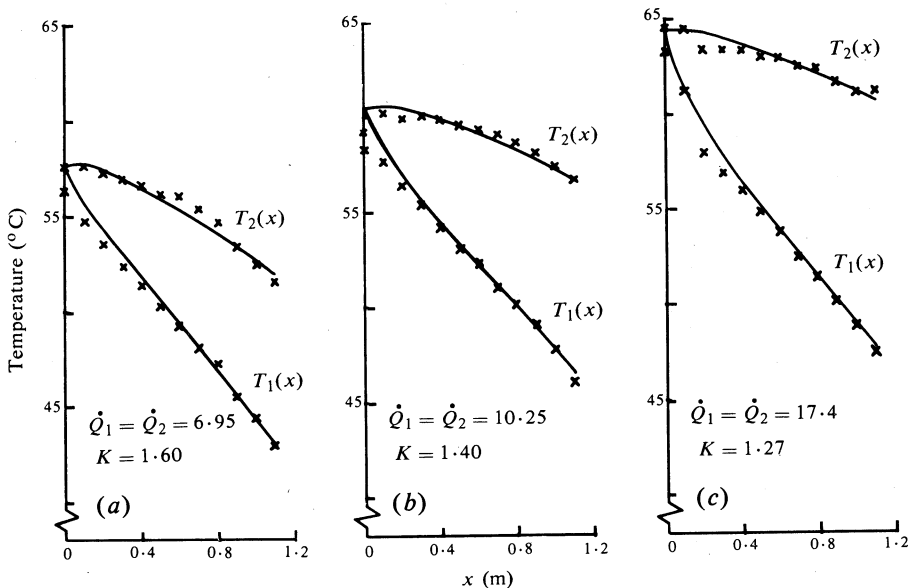


Fig. 12. Upper and lower stream fluid temperatures measured in the electrically heated stainless-steel riser depicted in Fig. 9. The riser was inclined at 24° to the horizontal. Results for three heat fluxes are shown along with the predictions of equation (22) and (23). Fitted parameters are listed in Table 1.

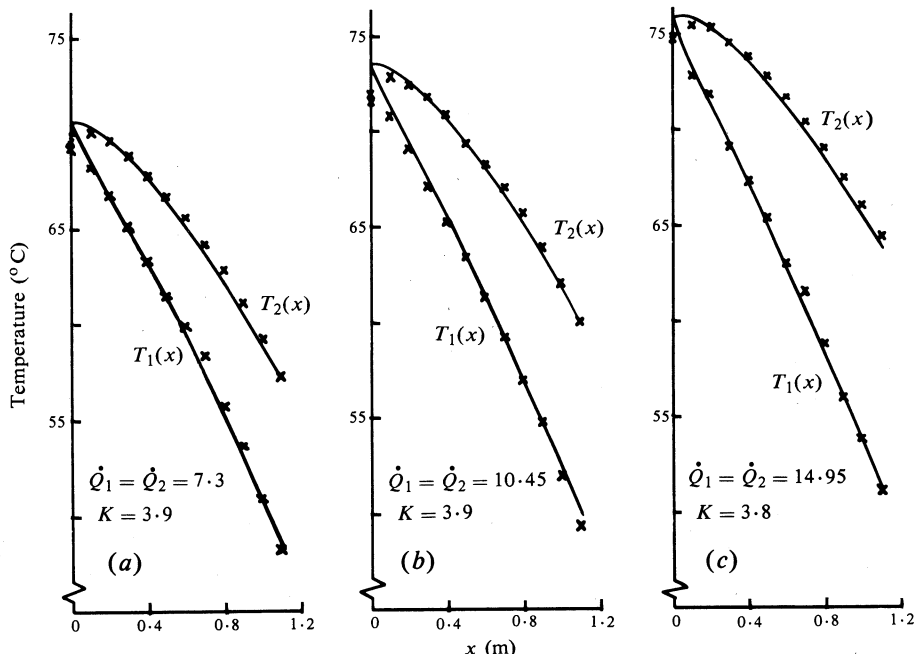


Fig. 13. Temperature profiles for an electrically heated copper riser mounted as in Fig. 9. Results are compared with equations (22) and (23) for three flux levels.

the cell. Typical maximum velocities of order 1 cm s^{-1} were observed, consistent with the observed mass fluxes of $4\text{--}6 \text{ g s}^{-1}$.

The cross cell temperature profile with symmetric heating is shown in Fig. 14*b* for two representative positions along the cell. The temperature gradients at the top and bottom boundaries are consistent with the constant heat flux boundary condition. The average stream temperatures, relevant to the model of Section 3, are approximated by the temperatures measured 2 mm from the boundaries. This leads to a possible underestimate of $T_1(x)$, particularly for large x , in the present case of symmetric heating. For many practical cases $\dot{Q}_1 < \dot{Q}_2$, so that these errors will be less significant.

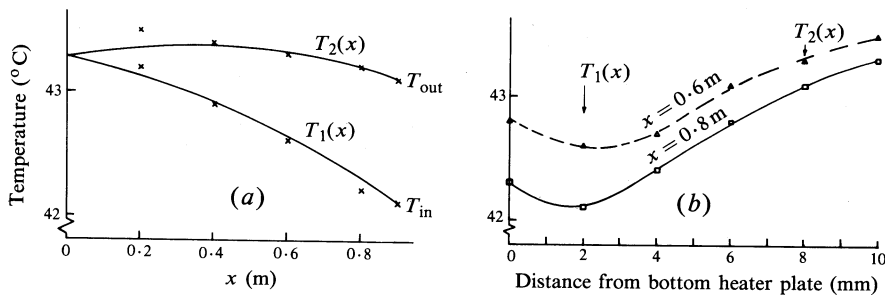


Fig. 14. Temperature profiles measured in the rectangular convection cell (Fig. 10) with heat exchanger temperature 38.1°C and symmetric heating ($\dot{Q}_1 = \dot{Q}_2 = 13 \text{ W}$): (a) longitudinal and (b) transverse temperature profiles. The average stream temperature is approximated by that measured 2 mm from top and bottom heater plates, as illustrated in (b). A constant mass flux $\dot{m} = 6.2 \text{ g s}^{-1}$ and $K = 35 \text{ W}^{\circ}\text{C}^{-1}$ yields the predicted curves for $T_1(x)$ and $T_2(x)$ shown in (a).

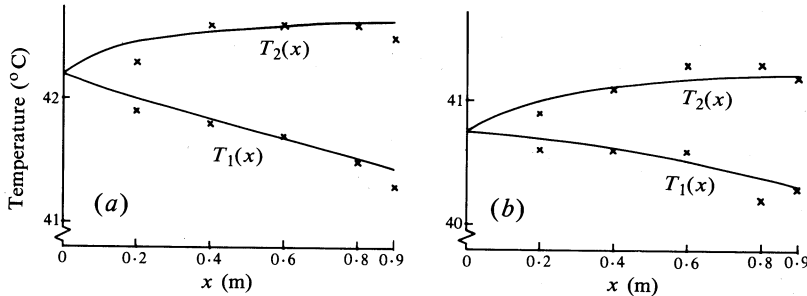


Fig. 15. Temperatures measured in the convection cell with asymmetric heating: (a) $\dot{Q}_1 = 4.8 \text{ W}$, $\dot{Q}_2 = 17.5 \text{ W}$ and $K = 5.2 \text{ W}^{\circ}\text{C}^{-1}$; (b) $\dot{Q}_1 = 0$, $\dot{Q}_2 = 20.2 \text{ W}$ and $K = 15.6 \text{ W}^{\circ}\text{C}^{-1}$. Other parameters are listed in Table 1. Temperatures predicted by equations (6) and (8) are shown by the curves.

A further issue highlighted by Fig. 14*b* is that a colder fluid layer (at about 2 mm) overlays the hotter fluid boundary layer adjacent to the bottom heater fluid. The Rayleigh number relevant only to this local stratification is of order 70, significantly less than the critical Rayleigh number (of order 10^3) for the onset of Rayleigh–Bénard convection. Thus, to leading order, the fluid stratification appears to be convectively stable. Note, however, that for the overall flow the Rayleigh number is $10^4\text{--}10^5$, approaching the transition to turbulent convection (Elder 1965*b*; Gill 1966).

For symmetric heating we observe that \dot{m} is approximately constant. The theoretical longitudinal temperature profiles, now calculated using (6) and (8), are shown in Fig. 14a with fitted K values. However, with asymmetric heating \dot{m} is not constant and the experimental values must be used, as shown in Fig. 15. At present we have no convincing explanation for the trends evident, but nevertheless our simple model is able to predict reasonably well temperature profiles for a range of thermosiphoning flows given the experimental $\dot{m}(x)$ and one adjustable parameter.

We have not investigated flows in the convection cell with $\dot{Q}_2 = 0$ since this corresponds to the Rayleigh-Bénard experiment (fluid heated from below) and is of less relevance to solar systems.

Thermosiphoning flows in the rectangular convection cell were also investigated at higher heat fluxes, up to 7 kW m^{-2} . However, even at heat fluxes only slightly greater than those in Figs 14 and 15, individual temperature readings indicated rapid fluctuations. Time averaged temperature readings must then be used. At higher heat fluxes a quasi-periodic and, ultimately, highly disordered temperature time dependence was evident. In addition, macroscopically coherent fluctuations were occasionally observed. Our simple model is clearly unsuited to these regimes.

6. Discussion and Conclusions

A feature of this work is the physical insight that a simple, essentially two-dimensional, analysis provides when applied to the combined heat and mass flow characteristics of a complex three-dimensional system. The analysis deals with averages of the temperature, and fluid flow over each of two counter-flowing streams, but is able to predict quantitatively the longitudinal temperature profiles in the liquid filled risers. Moreover, the model provides a method of estimating the magnitude of the heat flux between the streams, in very good agreement with experiment. For the cylindrical riser, at least, the flow is not characterised by a constant mass flow rate. It should be possible to obtain a reasonable fit to the data using a constant \dot{m} and K as variable parameters but this is inconsistent with the physics of the system and is not pursued here. Our method, based on the simple empirical approximation to the cross tube flow (see equation 21), successfully describes a variety of thermosiphoning flows without resort to the full two-dimensional hydrodynamic equations.

The model, and the experimental results reported here, are relevant to this system when operating in a stable configuration; all flows are laminar and temperatures are independent of time. Standard hydrodynamic analysis permits an estimate to be made of the point at which instability commences. In our experiments, these are observed at considerably lower heat fluxes and fluid velocities than those predicted. We are unable at this time to comment on the significance of this observation. We note, however, that the study of instabilities in similar systems is an active field of research. It is our intention to extend the analysis and the experimental studies into this more complex domain. It is also worth noting that the cylindrical riser is considerably more stable than the cell with planar geometry for comparable heat fluxes at the wall. It is not known, however, whether this relates to the stabilising influence of the greater surface area relative to riser volume, or to other factors.

Further work on this system will study the effect of different geometries, riser dimensions and angles of inclination. Previous work indicated that the heat transfer properties of this system are insensitive to angle, although the analysis must break

down for horizontal and vertical situations. The combination of this study with instability effects should prove fruitful. We also plan to develop a boundary layer analysis of the fluid flow in order to predict temperature profiles across the risers. Such results will be directly comparable with the experimental data reported here. The theoretical analysis should however, provide insights into the limitations of this heat transfer system.

Finally, comment needs to be made on the practical significance of a liquid filled riser as a heat transfer device. Our original intention was to use this system as a method of extracting heat from evacuated tubular solar collectors. It is clear that appropriately designed liquid filled risers can perform this function very well, having a thermal conductance up to 50 times that of a solid copper rod of the same diameter. This is within a factor of 2–4 of the performance of a heat pipe. The unexpected result is that the system works better with a wall material of poor thermal conductance, but is readily understood in terms of the model developed. The high thermal conductivity copper tube acts as a thermal short circuit around the tube, providing an additional path for heat transfer between the streams. Higher values of K are therefore observed under these conditions. The temperature profile across the riser will also change, which may then have an influence on the effective thermosiphoning pressure head and thus on the mass flow. Indeed, data indicate slightly lower mass flow rates for copper risers than for stainless steel, a point that warrants further study.

The utility of the riser system in evacuated tubular collectors will almost certainly depend on factors other than its heat transfer characteristics. Such factors include, for example, susceptibility to freezing, deposition of scale from potable water, effectiveness of heat transfer from the inner glass tube to the riser wall and, perhaps most importantly, cost.

Acknowledgments

The financial support of His Royal Highness Prince Nawaf bin Abdul Aziz of the Kingdom of Saudi Arabia through the Science Foundation for Physics is gratefully acknowledged. Expert technical assistance was provided by S. Farrar, H. Haldane, D. Hilliger, D. Kelly, D. Mackey and S. O'Shea.

References

- Baker, D. J. (1966). *J. Fluid Mech.* **26**, 573–5.
- Batchelor, G. K. (1954). *Q. J. Mech. Appl. Maths.* **12**, 209–33.
- Bénard, H. (1901). *Ann. Chim. Phys.* **23**, 62–144.
- Boussinesq, J. (1903). ‘Theorie Analytique de la Chaleur’, Vol. 2, p. 172 (Gauthier-Villars: Paris).
- Crevelling, H. F., De Paz, J. F., Baladi, J. Y., and Schoenhals, B. J. (1975). *J. Fluid Mech.* **67**, 65–84.
- Elder, J. W. (1965a). *J. Fluid Mech.* **23**, 77–98.
- Elder, J. W. (1965b). *J. Fluid Mech.* **23**, 99–111.
- Gebhart, B. (1971). ‘Heat Transfer’ (McGraw-Hill: New York).
- Gill, A. E. (1966). *J. Fluid Mech.* **26**, 515–36.
- Gorman, M., Widmann, P. J., and Robbins, K. A. (1984). *Phys. Rev. Lett.* **52**, 2241–4.
- Gorman, M., Widmann, P. J., and Robbins, K. A. (1986). *Physica D* **19**, 255–67.
- Grief, R., Zvirin, Y., and Mertol, A. (1979). *J. Heat Transfer* **101**, 684–8.
- Hansen, A. G. (1967). ‘Fluid Mechanics’ (Wiley: New York).
- Harding, G. L., and Window, B. (1979). *J. Vac. Sci. Technol.* **16**, 2101–4.
- Harding, G. L., Window, B., and Gammon, R. (1982). *Int. J. Ambient Energy* **3**, 171.
- Harding, G. L., and Yin, Z. Q. (1985). *Sol. Energy* **34**, 13–18.

- Harding, G. L., Yin, Z. Q., and Mackey, D. W. (1985). *Sol. Energy* **35**, 71–91.
- Hart, J. E. (1971). *J. Fluid Mech.* **47**, 547–76.
- Hart, J. E. (1984). *J. Fluid Mech.* **77**, 125–36.
- Hartnett, J. P., and Welsh, W. E. (1957). *Trans. Am. Soc. Mech. Eng.* **79**, 1551.
- Hasegawa, S., Nishihawa, K., and Yamagata, K. (1963). *Bull. Jap. Soc. Mech. Eng.* **6**, 230.
- Holman, J. P. (1981). 'Heat Transfer' (McGraw-Hill: New York).
- Huang, B. J. (1980). *Sol. Energy* **25**, 105–16.
- Jaluria, Y. (1980). 'Natural Convection Heat and Mass Transfer' (Pergamon: New York).
- Keller, J. B. (1966). *J. Fluid Mech.* **26**, 599–606.
- Kimura, S., and Bejan, A. (1984). *J. Heat Transfer* **106**, 98–103.
- Larsen, F. W., and Hartnett, J. P. (1961). *Heat Transfer C* **83**, 87.
- Lighthill, M. J. (1953). *Q. J. Mech. Appl. Math.* **6**, 398–439.
- Lorenz, E. (1963). *J. Atmos. Sci.* **20**, 130–41.
- Martin, B. W. (1955). *Proc. R. Soc. London A* **230**, 502.
- Martin, B. W., and Cohen, H. (1954). *Brit. J. Appl. Phys.* **5**, 91.
- Mertol, A., Grief, R., and Zvirin, Y. (1982). *J. Heat Transfer* **104**, 508–14.
- Mertol, A., Place, W., Webster, T., and Grief, R. (1981). *Sol. Energy* **27**, 367–86.
- Mihaljan, J. (1962). *Astrophys. J.* **136**, 1126–33.
- Ostrach, S. (1972). *Adv. Heat Transfer* **8**, 161–227.
- Rayleigh, Lord (1916). *Philos. Mag.* **32**, 529–46.
- Roache, P. J. (1972). 'Computational Fluid Dynamics' (Hermosa: Alburquerque).
- Schmid, R., and Collins, R. E. (1985). Abstract, ISES, Montreal, 'Intersol 85' (Eds E. Bilger and K. G. T. Hollands) (Pergamon: New York).
- Sen, M., Ramos, E., and Trevino, C. (1985). *Int. J. Heat Mass Transfer* **28**, 219–33.
- Turner, J. S. (1973). 'Buoyancy Effects in Fluids' (Cambridge Univ. Press).
- Welander, P. (1967). *J. Fluid Mech.* **29**, 17–30.
- Window, B. (1983). *Sol. Energy* **31**, 159–66.
- Window, B., and Harding, G. L. (1983). *Sol. Energy* **31**, 153–7.
- Window, B., and Harding, G. L. (1984). *Sol. Energy* **35**, 609–23.
- Yin, Z. Q., Harding, G. L., Craig, S., and Collins, R. E. (1985). *Sol. Energy* **35**, 81–91.
- Yin, Z. Q., Harding, G. L., and Window, B. (1984). *Sol. Energy* **32**, 223–30.

Manuscript received 29 May, accepted 26 June 1986

